

A simplified structure-based model using standard turbulence scale equations: computation of rotating wall-bounded flows

S.C. Kassinos^{a,b,*}, C.A. Langer^a, G. Kalitzin^b, G. Iaccarino^b

^a Department of Mechanical and Manufacturing Engineering, University of Cyprus, 75 Kallipoleos St., P.O. Box 20537, Nicosia 1678, Cyprus

^b Center for Turbulence Research, Stanford University, Stanford CA 94305, USA

Available online 31 March 2006

Abstract

Two linear eddy-viscosity models, the v^2-f and $k-\omega$ models, have been combined with an algebraic structure-based algorithm for the evaluation of the Reynolds stresses. This closure was originally designed as an integral part of the algebraic structure-based model (ASBM) to capture the turbulent anisotropy occurring in rotating wall bounded flows. It is shown that the algebraic structure-based evaluation of the Reynolds stresses can be used directly with *conventional* turbulence models sensitizing them to rotation. Significant improvement in the prediction of anisotropic turbulent flow can be achieved without an additional tuning of the closure coefficients.

The models are evaluated in spanwise rotating channel flow and in flat plate boundary layers. The sensitivity to the Reynolds and rotation numbers is investigated. The results are compared with DNS data.

© 2006 Elsevier Inc. All rights reserved.

Keywords: Rotation; Turbulence modeling; Structure based; Algebraic model; V2F; Near wall

1. Motivation and objectives

Linear eddy-viscosity models are known to be inaccurate in predicting the effect of strong streamline curvature and frame rotation. There is no shortage of modifications and adjustments proposed in the literature to correct their behavior. For example in the work by Shih et al. (1995) the $k-\epsilon$ model is modified by introducing coefficients in the ϵ -equation that depend on the shear rate and frame rotation. A more consistent redesigning of the ϵ -equation for flows with rotational effects has been proposed by Haire and Reynolds (2003). Another recent attempt by Durbin and Pettersson Reif (2001) consists in the modification of the eddy-viscosity coefficient (again by introducing dependency on the shear rate and frame rotation). In the latter case the justification for the choice of the selected func-

tional dependency comes from the study of solutions of second-moment models in the case of homogeneous rotating shear. Although these modifications are shown to provide encouraging predictions for simple flows with rotation (namely channel flows), their accuracy for more complex situations remains unclear. Differential Reynolds stress models, on the other hand, possess the obvious advantage that the turbulence production terms and the stress anisotropy are automatically accounted for. Unfortunately, the difficulties in modeling the stress redistribution terms and their inherent numerical stiffness make them not amenable to mainstream use in engineering calculations.

Algebraic Reynolds stress models have received a substantial amount of attention given the potential benefit of introducing stress anisotropy in the *controlled* environment of an eddy-viscosity closure. Several models have been devised with various degree of success (Gatski and Speziale, 1993; Wallin and Johansson, 2002). The basic idea behind these models is to express the Reynolds stress tensor as a function of one or more (up to ten) different tensors. This is not different from what is used to derive the so-called non-linear eddy-viscosity models where additional

* Corresponding author. Address: Department of Mechanical and Manufacturing Engineering, University of Cyprus, 75 Kallipoleos St., P.O. Box 20537, Nicosia 1678, Cyprus. Tel.: +357 22 892296; fax: +357 22 892254.

E-mail address: kassinos@ucy.ac.cy (S.C. Kassinos).

(high-order) terms are added to the Boussinesq relationship between mean strain and Reynolds stresses. Reynolds and coworkers (see Reynolds, 1991; Kassinos and Reynolds, 1994; Kassinos et al., 2001) have repeatedly argued that for adequate modeling and description of rotating turbulence, information about the turbulence structure is crucial. The Reynolds stresses only characterize the componentality of turbulence, i.e., which velocity components are more energetic. The turbulent field has much more information than that contained in the Reynolds stresses, which is important in presence of rotation, and which is described by the turbulence structure. For instance, the dimensionality of the flow is important. This carries information about which directions are favored by the more energetic turbulent eddies: if the turbulent eddies are preferentially aligned with a given direction, then the dimensionality is smaller along that direction. In the algebraic structure-based model (ASBM), hypothetical turbulent eddies are used to bring awareness of turbulence structure into the turbulence model. Averaging over an ensemble of eddies produces a set of one-point statistics, representative of the eddy field, and a set of equations of state relating the Reynolds stresses to these statistics.

The structure-based approach to build the Reynolds stress closure has led in Langer and Reynolds (2003) to the development of an ASBM in conjunction with a novel two-equation model based on the transport equation for turbulent kinetic energy, k , and large scale vorticity ω^2 . The model has been calibrated for channel flow simulations and the results have shown excellent agreement with available DNS data.

The primary objective of this work was to implement the ASBM in a three-dimensional Reynolds-averaged Navier–Stokes (RANS) solver to perform simulations of complex flows. In this work we combine the ASBM Reynolds stress evaluation with conventional turbulence models, namely the k – ω and v^2 – f models. Results are presented for channel flow with and without spanwise rotation. Additionally, the combination of the ASBM with the v^2 – f scale equations was explored in boundary layer flows, now using a parabolic flow solver. To achieve the primary objective some modifications to the original ASBM formulation have been developed to ease its numerical implementation. In particular, a scalar diffusivity has been introduced to the transport equations of the turbulent scalars and a generalization of the blocking length scale definition has been introduced.

2. The turbulence structure tensors

Turbulence structure tensors can be formally defined as in Kassinos and Reynolds (1994) and Kassinos et al. (2001). They introduce the turbulent stream-function vector, ψ'_k , to explore and elaborate concepts of turbulence structure. From the ψ'_k definition it follows that the vector stream function at one point is determined by the vorticity at all points through a Poisson equation

$$u'_i = \epsilon_{ijk} \frac{\partial \psi'_k}{\partial x_j}, \quad \frac{\partial \psi'_k}{\partial x_k} = 0, \quad \Rightarrow \quad \frac{\partial^2 \psi'_i}{\partial x_k \partial x_k} = -\omega'_i. \quad (1)$$

The turbulence structure tensors are defined in terms of one point correlations of vector stream function gradients, and hence they contain non-local information about the turbulence

$$R_{ij} = \overline{u'_i u'_j} = \epsilon_{ist} \epsilon_{jprq} \frac{\partial \psi'_t}{\partial x_s} \frac{\partial \psi'_q}{\partial x_p}, \quad (2)$$

$$D_{ij} = \frac{\partial \psi'_k}{\partial x_i} \frac{\partial \psi'_k}{\partial x_j}, \quad F_{ij} = \frac{\partial \psi'_i}{\partial x_k} \frac{\partial \psi'_j}{\partial x_k},$$

where R_{ij} , D_{ij} , and F_{ij} are respectively the Reynolds stress, the structure dimensionality, and the structure circularity tensors. D_{ij} and F_{ij} carry information about the large-scale, energy-bearing, structure of the turbulence not conveyed by R_{ij} . R_{ij} measures the componentality of the turbulence. If the turbulence has one zero component (say $u'_3 = 0$), then it is *two-component* (2C), but it is not necessarily two-dimensional (2D). If none of the vector stream function components varies with x_1 , then $D_{11} = 0$, indicating that the turbulence is 2D and independent of x_1 . It need not be 2C when it is 2D. Similarly, if the large-scale vorticity is entirely aligned with the x_1 axis, then all F_{ij} other than F_{11} are zero.

For homogeneous turbulence, the contractions of the structure tensors are all twice the turbulent kinetic energy, $R_{ii} = D_{ii} = F_{ii} = q^2 = 2k$. Normalized structure tensors are then defined as

$$r_{ij} = R_{ij}/q^2, \quad d_{ij} = D_{ij}/q^2, \quad f_{ij} = F_{ij}/q^2. \quad (3)$$

Moreover, for homogeneous turbulence, there is a constitutive relationship among the tensors,

$$r_{ij} + d_{ij} + f_{ij} = \delta_{ij}. \quad (4)$$

Thus only two of the tensors are linearly independent. This suggests that it could be difficult to model turbulence in terms of a single one of them as one hopes to do in Reynolds stress transport modeling.

Kassinos et al. (2000) and Poroseva et al. (2002) solve transport equations for the different structure tensors. However, there are many tensor components, thus many transport equations. A simpler approach is sought to bring in the key structural physics. Here we model the structure tensors using the simpler concept of turbulent eddies.

3. The structure-based algebraic stress model

The eddy-axis concept (Kassinos and Reynolds, 1994) is used to relate the Reynolds stress and the structure tensors to parameters of a hypothetical turbulent eddy field. Each eddy represents a two-dimensional turbulence field, and is characterized by an eddy-axis vector, a_i . The turbulent motion associated with this eddy is decomposed in a component along the eddy axis, the jetal component, and a component perpendicular to the eddy axis, the vortical component. This motion can be further allowed to be flat-

tened in a direction normal to the eddy axis (a round eddy being characterized by a random distribution of kinetic energy around its axis). Averaging over an ensemble of turbulent eddies gives statistical quantities representative of the eddy field, along with constitutive equations relating the normalized Reynolds stresses, r_{ij} , and turbulence structure to the statistics of the eddy ensemble,

$$r_{ij} = \frac{\overline{u'_i u'_j}}{2k} = (1 - \phi) \frac{1}{2} (\delta_{ij} - a_{ij}) + \phi a_{ij} + (1 - \phi) \chi \left[\frac{1}{2} (1 - a_{nm} b_{mn}) \delta_{ij} - \frac{1}{2} (1 + a_{nm} b_{mn}) a_{ij} - b_{ij} + a_{in} b_{nj} + a_{jn} b_{ni} \right] + (-\gamma \Omega_k^T / \Omega^T) (\epsilon_{ipr} a_{pj} + \epsilon_{jpr} a_{pi}) \times \left\{ \frac{1}{2} [1 - \chi (1 - a_{nm} b_{mn})] \delta_{kr} + \chi b_{kr} - \chi a_{kn} b_{nr} \right\}, \quad (5)$$

$$d_{ij} = \frac{1}{2} (\delta_{ij} - a_{ij}) + \chi \left[-\frac{1}{2} (1 - a_{nm} b_{mn}) \delta_{ij} + \frac{1}{2} (1 + a_{nm} b_{mn}) a_{ij} + b_{ij} - (a_{in} b_{nj} + a_{jn} b_{ni}) \right], \quad (6)$$

where d_{ij} is the normalized dimensionality tensor.

The eddy-axis tensor, $a_{ij} = \langle V^2 a_{ij} \rangle$, is the energy-weighted average direction cosine tensor of the eddy axes. The eddy-axis tensor is determined by the kinematics of the mean deformation. Eddies tend to become aligned with the direction of positive strain rate, and they are rotated kinematically by mean or frame rotation.

Motion around the eddy is called vortical, and motion along the axis is called jetal. The eddy jetting parameter ϕ is the fraction of the eddy energy in the jetal mode, and $(1 - \phi)$ is the fraction in the vortical mode. Under irrotational mean deformation, eddies remain purely vortical ($\phi = 0$). Shear produces jetal eddies, and in the limit of infinite rapid distortion (RDT) $\phi \rightarrow 1$ for shear in a non-rotating frame. For shear in a rotating frame the limiting value of ϕ , under RDT, ranges from 1 for zero frame rotation to 0 for frame rotation that exactly cancels the mean rotation in the frame, for which the mean deformation in an inertial frame is irrotational.

The eddy helix vector γ_k arises from the correlation between the vortical and jetal components. Hence $\gamma_k = 0$ for purely vortical turbulence ($\phi = 0$) or for purely jetal turbulence ($\phi = 1$). Typically γ_k is aligned with the total rotation vector Ω_k^T . The eddy-helix vector is the key factor in setting the shear stress in turbulent fields.

Flattening is used to describe the degree of asymmetry in the turbulent kinetic energy distribution around an eddy. A round eddy has no preferential distribution. If the motion is not axisymmetric around the eddy axis, the eddy is called flattened. The eddy-flattening tensor, b_{ij} , is the energy-weighted average direction cosine tensor of the flattening vector. The intensity of the flattening is given by the flattening parameter, χ . Under rapid irrotational deformation in a

fixed frame eddies remain axisymmetric. Rotation tends to flatten the eddies in planes perpendicular to the rotation direction.

Following Reynolds et al. (2000), the eddy-axis tensor, a_{ij} , is computed on the analysis frame, where the turbulence might be at equilibrium or very close to it. The eddy-axis tensor is computed with no reference to the frame rotation, as it is only kinematically rotated by it (Kassinos and Reynolds, 1994; Haire and Reynolds, 2003). The evaluation is divided in two parts. Initially a strained eddy-axis tensor, a_{ij}^s , is evaluated based on the irrotational part of the mean deformation. Next a rotation operation is applied, sensitizing the eddy-axis tensor to mean rotation. This procedure produces eddy-axis tensor states that mimic the limiting states produced under RDT for different combinations of mean strain with on-plane mean rotation, while guaranteeing realizability of the eddy-axis tensor.

The strained a_{ij}^s is given by

$$a_{ij}^s = \frac{1}{3} \delta_{ij} + \frac{(S_{ik}^* a_{kj}^s + S_{jk}^* a_{ki}^s - \frac{2}{3} S_{mn}^* a_{nm}^s \delta_{ij}) \tau}{a_0 + 2 \sqrt{\tau^2 S_{kp}^* S_{kq}^* a_{pq}^s}}, \quad (7)$$

where $S_{ij}^* = S_{ij} - S_{kk} \delta_{ij} / 3$ is the traceless strain-rate tensor with $S_{ij} = (\partial u_i / \partial x_j + \partial u_j / \partial x_i) / 2$, τ is a time scale (Eq. (21)), and $a_0 = 1.6$ is a “slow” constant. This gives realizable states for the eddy-axis tensor under irrotational deformations.

The final expression for the homogeneous eddy-axis tensor, a_{ij} (for near-wall regions see Eq. (13)), is obtained by applying a rotation transformation to the strained eddy-axis tensor, a_{ij}^s ,

$$a_{ij} = H_{ik} H_{jl} a_{kl}^s, \quad H_{ij} = \delta_{ij} + h_1 \frac{\Omega_{ij}}{\sqrt{\Omega_{pp}^2}} + h_2 \frac{\Omega_{ik} \Omega_{kj}}{\Omega_{pp}^2}, \quad (8)$$

where $\Omega_{pp}^2 = \Omega_{pq} \Omega_{pq}$, and Ω_{pq} is the mean rotation rate tensor. The orthonormality conditions $H_{ik} H_{jk} = \delta_{ij}$ and $H_{ki} H_{kj} = \delta_{ij}$ require

$$h_1 = \sqrt{2h_2 - h_2^2 / 2}, \quad (9)$$

h_2 is determined with reference to RDT for combined homogeneous plane strain and rotation (see Reynolds et al., 2000; Haire and Reynolds, 2003),

$$h_2 = \begin{cases} 2 - 2\sqrt{\frac{1}{2}(1 + \sqrt{1-r})} & \text{if } r \leq 1 \\ 2 - 2\sqrt{\frac{1}{2}(1 - \sqrt{1-1/r})} & \text{if } r \geq 1 \end{cases}, \quad (10)$$

where $r = (a_{pq} \Omega_{qr} S_{rp}^*) / (S_{kn}^* S_{nm}^* a_{mk})$.

The flattening tensor b_{ij} is modeled in terms of the mean rotation rate vector, Ω_i , and the frame rotation rate vector, Ω_i^f ,

$$b_{ij} = \frac{(\Omega_i + C_b \Omega_i^f) (\Omega_j + C_b \Omega_j^f)}{(\Omega_k + C_b \Omega_k^f) (\Omega_k + C_b \Omega_k^f)}, \quad C_b = -1.0. \quad (11)$$

The helix vector γ_k is taken as aligned with the total rotation vector,

$$\gamma_k = \gamma \frac{\Omega_k^T}{\sqrt{\Omega_p^T \Omega_p^T}}, \quad \gamma = \beta \sqrt{\frac{2\phi(1-\phi)}{1+\chi}}. \quad (12)$$

Modeling ϕ , β (see Eq. (12)), and χ is a crucial part in the construction of the model. The equations for these scalars are found by analyzing target turbulent states corresponding to a mean deformation. Throughout model development there is a strong effort to make it consistent with RDT solutions, aiming to improve model dependability and realizability for a wide range of mean deformations, as well as to obtain guidance in the functional shape chosen for the structure parameters. Tentative functional forms for the structure parameters are thus chosen with reference to RDT. A set of structure parameter values is chosen to mimic the isotropic turbulent state (the eddy structure is expected to consist of axisymmetric ($\chi=0$), vortical ($\phi=0$) eddies). Finally interpolation functions (along with model constants) are chosen to bridge these limiting states (isotropy and RDT). They are selected specially to match a canonical state of sheared turbulence, observed in the log region of a boundary layer. In the resulting model the structure scalars are parameterized in terms of η_m , η_f , and a^2 , representatives of the ratio of mean rotation to mean strain, frame rotation to mean strain, and a measure of anisotropy respectively. Details are given in Appendix.

As a no-slip wall is approached, the velocity is driven to zero through the action of viscous forces. Furthermore, the velocity vector is reoriented into planes parallel to the wall through an inviscid mechanism (wall blocking) which acts over distances far larger than the viscous length scale. Thus the velocity component normal to the wall is driven to zero faster than the tangential components. In the structure-based model it is postulated that the eddy orientation shall also be parallel to the wall. A wall-blocking procedure is then introduced to reorient the eddies. The structure parameters are also sensitized to wall blocking, such that the modeled Reynolds stresses are consistent with the expected near wall asymptotic behavior.

Following Reynolds et al. (2000), the homogeneous eddy-axis tensor, a_{ij}^h , is computed based on the homogeneous algebraic procedure, Eqs. (7) and (8) (note that the superscript “h” has been added in the current section). It is then partially projected onto planes parallel to the wall,

$$a_{ij} = H_{ik} H_{jl} a_{kl}^h, \quad H_{ik} = \frac{1}{D_a} (\delta_{ik} - B_{ik}), \quad (13)$$

$$D_a^2 = 1 - (2 - B_{kk}) a_{mn}^h B_{nm},$$

where H_{ik} is the partial-projection operator, and D_a^2 is such that the trace of a_{ij} remains unity. The blockage tensor B_{ij} gives the strength and the direction of the projection. If the wall-normal direction is x_2 , then B_{22} is the sole non-zero component, and varies between 0 (no blocking) far enough from the wall, to 1 (full blocking) at the wall. B_{ij} is computed by

$$B_{ij} = \frac{\Phi_{,i} \Phi_{,j}}{\Phi_{,k} \Phi_{,k}} \Phi \quad \text{if } \Phi_{,k} \Phi_{,k} > 0. \quad (14)$$

If all gradients of Φ vanish, the denominator in (14) has been clipped setting effectively B_{ij} to zero.

The blocking parameter, Φ , is computed by an elliptic relaxation equation

$$L^2 \frac{\partial^2 \Phi}{\partial x_k \partial x_k} = \Phi, \quad L = C_L \text{Max} \left(\frac{k^{3/2}}{\varepsilon}, C_v \sqrt{\frac{v^3}{\varepsilon}} \right) \quad (15)$$

with $\Phi = 1$ at solid boundaries, and $\Phi_{,n} \equiv \partial \Phi / \partial x_n = 0$ at open boundaries, where x_n is the direction normal to the boundary. The definition of L is inspired by Durbin and Pettersson Reif (2001). Here $C_v = 50$, and

$$C_L = 1.0 \frac{S\tau}{S^2 \tau^2 + 15} \quad (16)$$

with $S^2 = 2S_{ij}S_{ji}$. This form is chosen so as to limit the growth of L in rotating flows, when ε decreases substantially. An overgrown L would enforce too much blocking on the turbulence structure over too much of the flow. An alternative solution would follow Pettersson and Andersson (1997), and add the mean flow viscous dissipation to ε . This would in fact again limit the decay of ε near a stable wall in rotating flows.

To recover proper asymptotic behavior of the Reynolds stresses, $r_{12} \propto O(x_2)$ and $r_{22} \propto O(x_2^2)$, as the wall at $x_2 = 0$ is approached, the homogeneous jetal, ϕ^h , and helix, γ^h , parameters are modified using

$$\phi = 1 + (\phi^h - 1)(1 - B_{kk})^2, \quad (17)$$

$$\gamma = \gamma^h(1 - B_{kk}). \quad (18)$$

A consequence of this approach is that realizability is automatically satisfied for r_{ij} .

4. Rotating channel flow and flat plate boundary layer computed with conventional turbulence models combined with ASBM

The steady RANS equations governing the motion of an incompressible viscous fluid in a Cartesian rotating frame of reference are given by conservation of mass and momentum as in Greenspan (1968):

$$\frac{\partial u_i}{\partial x_i} = 0, \quad (19)$$

$$u_j \frac{\partial u_i}{\partial x_j} + 2\epsilon_{ijk} \Omega_j^f u_k = -\frac{\partial P}{\partial x_i} + \nu \frac{\partial^2 u_i}{\partial x_k \partial x_k} + \frac{\partial}{\partial x_j} (\overline{-u_i' u_j'}), \quad (20)$$

where u_i is the mean velocity measured in the coordinate system rotating with constant angular velocity Ω_j^f , and x_j , P , ρ , and ν represent respectively the position vector, reduced pressure, density and kinematic viscosity. The reduced pressure incorporates the centripetal acceleration.

For fully-developed channel flow in a spanwise rotating frame the mean velocity is given by $u_j = u(y)$ where y is the

wall normal direction. The frame rotation rate vector is given by $\Omega_j^f = \Omega^f \delta_{j3}$ with x_3 being the spanwise direction. The wall-normal mean velocity component vanishes by continuity for a fully-developed channel flow with zero velocity at the walls. This simplifies the momentum equation; only the streamwise direction component, x , needs to be solved and the term containing the angular velocity Ω^f is zero.

The Reynolds stress in Eq. (20) is obtained through the algebraic equation (5). The complete ASBM model, described in Langer and Reynolds (2003), includes two scalar transport equations for the turbulent kinetic energy k and the large-scale turbulent enstrophy ω^2 . The purpose of these two quantities is to provide the field distribution of k and of the turbulence time scale τ . The latter has the following relation to k and ϵ :

$$\tau^2 = \left(\frac{k}{\epsilon}\right)^2 + \left(2.0\sqrt{\frac{\nu}{\epsilon}}\right)^2. \quad (21)$$

In this work, field distributions of k and τ have been obtained from the k - ω model by Wilcox (1993) and v^2 - f model by Lien and Durbin (1996). In addition, low- Re modifications given in Wilcox (1993) for the k - ω model have been considered. For the k - ω model, the time scale is computed as $\tau^2 = 1/(\beta^*\omega)^2 + 4.0\nu/(k\omega\beta^*)$ while Eq. (21) is used directly for v^2 - f which includes transport equations for k and ϵ .

The time scale is used to scale the rotation rate tensor, Ω_{ij} , and strain rate tensor, S_{ij} , that are obtained from the mean flow velocity distribution. The blockage tensor B_{ij} is obtained as described above from an elliptic equation. The tensors τS_{ij} , $\tau \Omega_{ij}$ and B_{ij} as well as k and τ and the frame rotation vector $\tau \Omega_j^f$ provide the necessary information for the ASBM Reynolds stresses $\tau_{ij} = -\overline{u_i' u_j'}$.

Following Eq. (20), the Reynolds stress enters only the diffusion term in the momentum equation. In an incompressible RANS flow solver based on a standard SIMPLE algorithm the diffusion term is usually treated implicitly for stability. This is straightforward when the Reynolds stress is computed over the Boussinesq approximation and an eddy-viscosity is used. With the ASBM procedure the Reynolds stress is computed explicitly and an explicit correction to the momentum equation is used. For the implementation of the ASBM procedure in the IBRANS code by Kalitzin and Iaccarino (2003) the last two terms in Eq. (20) have been re-written as

$$\frac{\partial}{\partial x_j} \left[(v + v_r^n) \frac{\partial u_i^{n+1}}{\partial x_j} \right] - \frac{\partial}{\partial x_j} \left[v_r^n \frac{\partial u_i^n}{\partial x_j} - \tau_{ij}^n \right], \quad (22)$$

where n is the current iteration. The terms with the eddy-viscosity are equal to each other when the solution is converged. The eddy-viscosity used is as defined by the k - ω or v^2 - f model.

The Reynolds stress enters only the production term $P_k = \tau_{ij} \hat{\omega}_{ij} \partial x_j$ in the transport equations of the turbulence models. The eddy-viscosity is retained in the diffusion terms

and no additional modifications of the turbulence equations have been performed in respect to the frame rotation.

Haire and Reynolds (2003) also looked at using alternative scale equations along with an earlier version of the ASBM, for free shear flows. A few distinctions are present in the current investigation. Briefly, (i) the turbulent transport term in the scale equations has a tensorial form in Haire and Reynolds (2003), whilst here a scalar diffusion model is investigated, for its simplicity makes it possible to use the ASBM in available CFD packages, (ii) Haire and Reynolds concentrated on free shear flows. The analysis here regards wall-bounded flows, and (iii) the algebraic equations that constitute the current ASBM formulation are different from the earlier version explored by them.

The channel flow computations have been performed considering a streamwise periodic flow with one cell in the flow direction. The pressure and velocity components at the outflow have been copied to the inflow and a source term has been added to the momentum equation to account for the pressure loss.

Finally, a parabolic flow solver was introduced to compute two flat plate boundary layers: Spalart (1988) zero pressure gradient (ZPG) at $Re_\theta = 1410$, and Spalart and Watmuff (1993) adverse pressure gradient (APG) boundary layer.

5. Numerical results

Channel flow simulations in orthogonal mode rotation have been performed for a variety of Reynolds and rotation numbers. The first objective of these simulations is to identify the steps necessary to combine the ASB Reynolds stress evaluation and a *conventional* eddy-viscosity model. As shown earlier the RANS equations are *closed* when the eddy-viscosity is introduced; therefore, the first, preliminary, step is to use the ASB procedure as a post-processing tool to evaluate the Reynolds stresses. Successive steps consist of introducing different levels of coupling between ASB and the overall solution procedure; first, only the mean equations are modified by discarding the eddy-viscosity and evaluating the divergence of the Reynolds stresses directly. Finally, a fully coupled solution is obtained when the Reynolds stresses are also used to close terms in the equations for turbulent quantities. The results obtained are summarized in Fig. 1 for the k - ω and the v^2 - f models in a channel flow without rotation. Not surprisingly, the best match with the experiments is obtained when the full coupling is employed; it is also very interesting to note that the use of ASB as a post-processing is already sufficient to obtain the correct level of anisotropy as opposed to the standard application of the eddy-viscosity models. This situation is clearly a peculiarity of this specific test case because the stress anisotropy does not affect the mean flow transport. Another important observation is that the inclusion of the ASB stress evaluation in the turbulent kinetic energy production is necessary to obtain accurate results. It must be noted that in the original ASBM

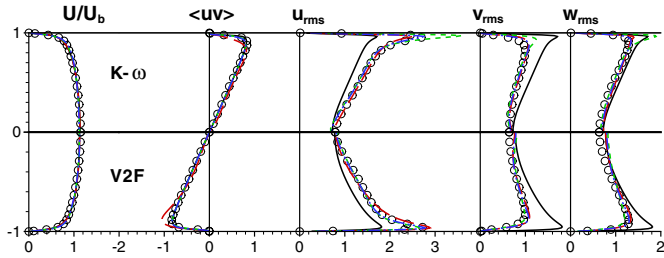


Fig. 1. Channel flow at $Re = 395$ computed with low- Re $k-\omega$ (upper half) and v^2-f (lower half) models as: —: Reynolds stress computed from Boussinesq approximation for linear model, - -: ASB Reynolds stress from linear model, ---: ASB Reynolds stress used only in the mean flow, - · - ·: ASB Reynolds stress used in the mean flow and in the production term of models, \circ : DNS by Moser et al. (1999).

approach by Langer and Reynolds (2003), a tensorial turbulent diffusivity is also included whereas in the present implementation a scalar coefficient is used.

Fig. 2 shows the effect of the Reynolds number for flow without rotation. In this case the high- and low- Re ASB $k-\omega$ as well as the ASB v^2-f models are reported. Here we added the ASB prefix to the models to indicate that the Reynolds stresses are evaluated with the ASB procedure. The latter two produce results that are satisfactory for both Reynolds numbers whereas the high- Re ASB $k-\omega$ underpredicts the peak of the u_{rms} in particular for $Re = 180$.

The application of the fully-coupled approach for the flow in a channel with rotation is reported in Figs. 3 and 4 for a channel flow at two different rotation numbers. The rotation number is defined here as $Ro = \Omega^f 2h/u_b$ where Ω^f is the magnitude of the frame rotation rate, h is the half-

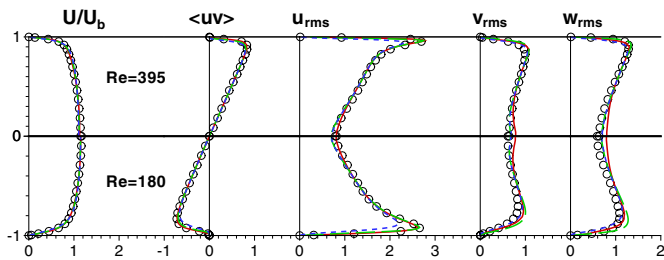


Fig. 2. Channel flow at $Re = 395$ (upper half) and $Re = 180$ (lower half). —: ASB v^2-f , - -: ASB low- Re $k-\omega$, ---: ASB high- Re $k-\omega$, \circ : DNS by Moser et al. (1999).

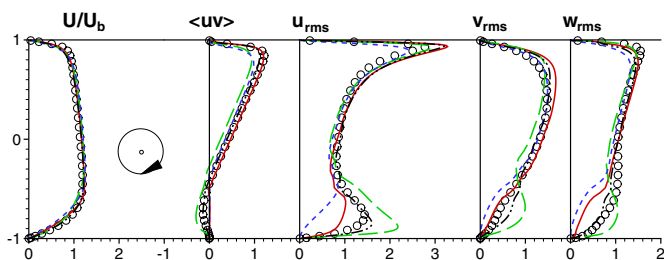


Fig. 3. Rotating channel flow at $Re = 180$ and $Ro = 0.22$. —: ASB v^2-f , - -: ASB low- Re $k-\omega$, ---: ASB high- Re $k-\omega$, - · - ·: ASBM, \circ : DNS by Alvelius (1999).

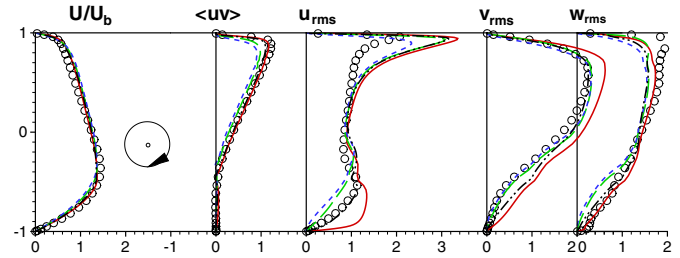


Fig. 4. Rotating channel flow at $Re = 180$ and $Ro = 0.77$. —: ASB v^2-f , - -: ASB low- Re $k-\omega$, ---: ASB high- Re $k-\omega$, - · - ·: ASBM, \circ : DNS by Alvelius (1999).

height of the channel and u_b is the bulk velocity in the channel. In these plots DNS data and the original ASBM are compared to ASB $k-\omega$ and ASB v^2-f predictions. The asymmetry in the mean velocity profile is properly captured even for the high rotation case. In addition, the Reynolds stress anisotropy is remarkably close to the DNS results at the turbulence-enhanced side of the channel. Notice that at the suction-side of the channel (lower side in the Figs. 3 and 4) the turbulence intensity is reduced and, eventually, the turbulent stresses are negligible with respect to the viscous stresses. The difference between the full ASBM approach and the current combined approach is also very small especially when v^2-f is used.

Further simulations have been performed at a variety of rotation numbers in the $[0-0.77]$ interval. The results obtained using the v^2-f and the ASB v^2-f are presented. The mean velocity profile and the turbulent kinetic energy are reported in Figs. 5 and 6, respectively. The current model and the DNS again agree remarkably well.

Fig. 7 illustrates the behavior of the normalized structure dimensionality in the channel flow. It is not used in the present computations, but it is nevertheless instructive to observe its behavior. In the left, for the fixed frame channel, the model compares favorably with DNS results, especially in the region away from the wall. The behavior of the d_{11} component is particularly encouraging. It is the smallest component, indicating the presence of structures preferentially aligned with the streamwise (x_1) direction. Furthermore it shows a minimum near the wall, where near-wall streaks aligned with the flow direction have come to be expected. Comparing to the figure on the right, in a rotating channel, it is clear that the dimensionality is little affected by the frame rotation. It does display an asymme-

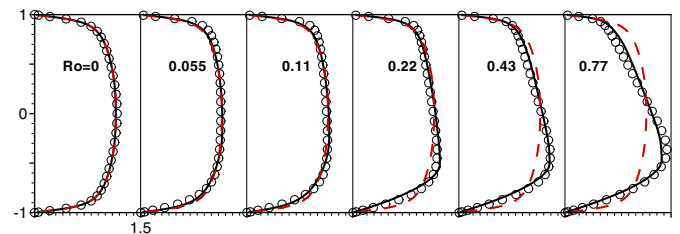


Fig. 5. Velocity profiles for channel flow at $Re = 180$ and $Ro = 0, 0.055, 0.11, 0.22, 0.43$ and 0.77 ; ---: v^2-f , —: ASB v^2-f , \circ : DNS by Alvelius (1999).

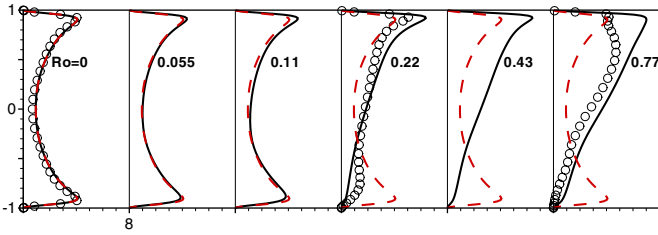


Fig. 6. Turbulent kinetic energy for channel flow at $Re = 180$ and $Ro = 0, 0.055, 0.11, 0.22, 0.43$ and 0.77 ; ---: v^2-f , —: ASB v^2-f , \circ : DNS by Alvelius (1999).

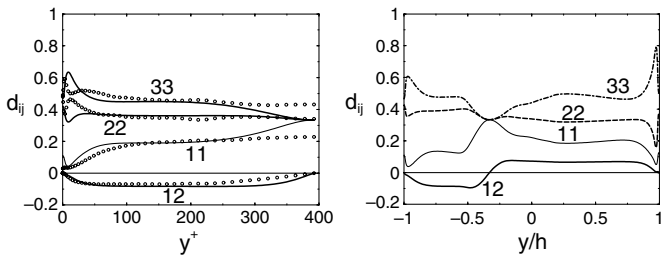


Fig. 7. Normalized structure dimensionality tensor components. Left: fixed frame channel flow at $Re = 385$. Right: spanwise-rotating channel flow at $Re = 360$ and $Ro = 0.22$; ---: ASB v^2-f , \circ : DNS by Kim (1992).

try, but this results directly from the asymmetry in the mean velocity gradient. There are no dramatic changes as in the Reynolds stresses.

Figs. 8 and 9 show comparisons of the ASB v^2-f with DNS of a ZPG boundary layer by Spalart (1988) and with DNS of an APG boundary layer by Spalart and Watmuff (1993), respectively. Comparisons are made using wall units, and in the APG case, only one station is reported, 2/3 of the way through what Spalart and Watmuff call

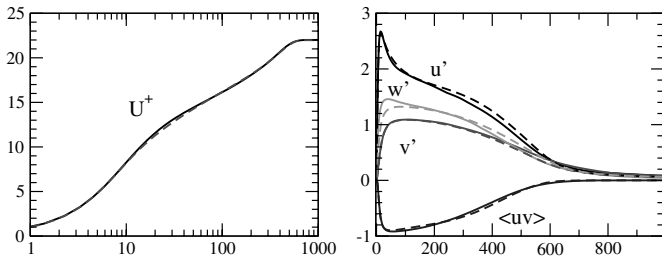


Fig. 8. ZPG boundary layer at $Re_\theta = 1410$; ---: ASB v^2-f , —: DNS by Spalart (1988).

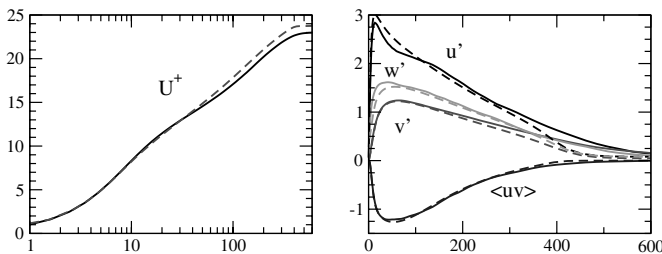


Fig. 9. APG boundary layer at $x = 0.80$; ---: ASB v^2-f , —: DNS by Spalart and Watmuff (1993).

the “comparison region”, $x = 0.80$. The anisotropies of the turbulence intensities predicted with the ASB v^2-f are in very good agreement with the DNS.

6. Conclusions and future plans

The algebraic structure-based model has been used in this work in combination with conventional linear eddy-viscosity models to evaluate the Reynolds stresses in the RANS equations. This approach has proven to be very accurate in predicting the mean flow and the stress anisotropy in rotating channel flow as opposed to the baseline eddy-viscosity predictions that are typically insensitive to frame rotation. Several modifications, that have not been reported in this paper, have been introduced to the ASBM model in order to facilitate its application to more general flow problems. In particular, a scalar turbulent diffusion coefficient is introduced in lieu of the original tensorial diffusivity, in the transport equations for the turbulence scalars k, ϵ , etc.

The current combination of the ASB Reynolds stress evaluation with the v^2-f and $k-\omega$ models is carried out in a full three-dimensional flow solver. However, only channel flow simulations were performed. Preliminary computations of flows in square-ducts appeared encouraging. Results for ZPG and APG boundary layer flows computed with a separate parabolic solver are also encouraging.

Acknowledgements

We thank Dr. Krister Alvelius and Professor Arne Johansson from KTH for kindly providing us with the rotating channel DNS data.

Appendix

The structure scalars ϕ, β , and χ , respectively the eddy jetting parameter, the eddy jetal-helix correlation parameter, and the eddy flattening parameter, are a crucial part in modeling the structure tensors. Langer and Reynolds (2003) discuss their construction in detail; the final forms are summarized here. They are parameterized in terms of η_m, η_f , and a^2 , representatives of the ratio of mean rotation to mean strain, frame rotation to mean strain, and a measure of anisotropy respectively. These in turn are defined in terms of $\widehat{\Omega}_m^2 \tau^2, \widehat{\Omega}_T^2 \tau^2$, and $\widehat{S}^2 \tau^2$; measures of the strength of the mean rotation, total rotation, and mean strain respectively. τ represents a time scale of the turbulence (Eq. (21))

$$\eta_m \equiv \sqrt{\frac{\widehat{\Omega}_m^2}{\widehat{S}^2}}, \quad \eta_f \equiv \eta_m - \text{sign}(X) \sqrt{\frac{\widehat{\Omega}_T^2}{\widehat{S}^2}}, \quad a^2 \equiv a_{pq} a_{pq},$$

$$\widehat{\Omega}_m^2 \equiv -a_{ij} \Omega_{ik} \Omega_{kj}, \quad \widehat{\Omega}_T^2 \equiv -a_{ij} \Omega_{ik}^T \Omega_{kj}^T,$$

$$\widehat{S}^2 \equiv a_{ij} S_{ik} S_{kj}, \quad X \equiv a_{ij} \Omega_{ik}^T S_{kj}.$$

The structure parameters are then defined with the help of auxiliary functions (see Table 1)

Table 1
Structure scalars: auxiliary functions in Eqs. (23)–(25)

$\eta_m = 1$	ϕ_1	β_1	χ_1
$\eta_f < 0$	$\frac{\eta_f - 1}{3\eta_f - 1}$	$\left[1 - b_0 \frac{\eta_f}{(1-a^2)} \left(1 + \sqrt{(a^2 - 1/3)}\right)\right]^{-1}$	$\frac{1}{2} \beta_1$
$0 < \eta_f < 1$	$(1 - \eta_f)$	1	$\frac{1}{2} + \frac{1}{2} \left[1 - \frac{(1-\eta_f)^2}{1+b_1\eta_f/(1-a^2)}\right]$
$\eta_f > 1$	$\frac{\eta_f - 1}{3\eta_f - 1}$	$\left[1 + b_2 \frac{(\eta_f - 1)}{(1-a^2)} \eta_f \sqrt{(a^2 - 1/3)}\right]^{-1}$	$1 - \frac{(1-\beta_1)(\eta_f - 1)}{b_3(1-a^2) + (\eta_f - 1)}$
$\eta_m = 0$	ϕ_0	β_0	χ_0
$\eta_f \leq \sqrt{3}/4$	$0.145 \left[\frac{(2\eta_f)^2}{3/4} - \left(\frac{(2\eta_f)^2}{3/4} \right)^9 \right]$	1	$-\left[0.342 \frac{(2\eta_f)^2}{3/4} + (1 - 0.342) \left(\frac{(2\eta_f)^2}{3/4} \right)^6\right]$
$\eta_f > \sqrt{3}/4$	$(1 + \chi_0)/3$	$-\chi_0$	$-\left[1 + b_4 \frac{(\eta_f - \sqrt{3}/4)}{(1-a^2)} \eta_f \sqrt{(a^2 - 1/3)}\right]^{-1}$
η_m	ϕ^*	β^*	χ^*
< 1	$\phi_0(\eta_*) + [\phi_1(\eta_*) - \phi_0(\eta_*)]\eta_m^2$	$\beta_0(\eta_*) + [\beta_1(\eta_*) - \beta_0(\eta_*)]\eta_m^2$	$\chi_0(\eta_*) + [\chi_1(\eta_*) - \chi_0(\eta_*)]\eta_m^4$
> 1	$1/3 + \frac{(\phi_1(\eta_f, a^2) - 1/3)}{1 + (\eta_m - 1)/(1-a^2)}$	$\frac{\beta_1(\eta_f, a^2)}{1 + (\eta_m - 1)/(1-a^2)}$	$\frac{\chi_1(\eta_f, a^2)}{1 + (\eta_m - 1)/(1-a^2)}$

$$b_0 = 1.0, b_1 = 100, b_2 = 0.8, b_3 = 1.0, b_4 = 1.0, \eta_* \equiv -\eta_m + [4/\sqrt{3} + (2 - 4/\sqrt{3})\eta_m]\eta_f.$$

$$\phi = \phi^* \times \left(\frac{(\eta_m - \eta_f)^2}{(\eta_m - \eta_f)^2 + (1 - a^2)^2} \right) \times \left(\frac{|\eta_m - \eta_f| \sqrt{\frac{3}{2}(a^2 - \frac{1}{3})}}{|\eta_m - \eta_f| \sqrt{\frac{3}{2}(a^2 - \frac{1}{3})} + p_0(1 - a^2)} \right), \quad (23)$$

$$\beta = \beta^*, \quad (24)$$

$$\chi = \chi^* \times \left[\frac{3}{2} \left(a^2 - \frac{1}{3} \right) \right]^{p_1}. \quad (25)$$

References

- Alvelius, K., 1999. Studies of turbulence and its modeling through large eddy and direct numerical simulation, Ph.D. Thesis, Department of Mechanics, KTH, Stockholm, Sweden.
- Durbin, P.A., Petterson Reif, B.A., 2001. Statistical Theory and Modeling for Turbulent Flows. John Wiley & Sons.
- Gatski, T.B., Speziale, C.G., 1993. On explicit algebraic stress models for complex turbulent flows. *J. Fluid Mech.* 254, 59–78.
- Greenspan, H.P., 1968. The Theory of Rotating Fluids. Cambridge University Press.
- Haire, S.L., Reynolds, W.C., 2003. Toward an affordable two-equation structure-based turbulence model, Technical Report TF-84, Mechanical Engineering Department, Stanford University.
- Kalitzin, G., Iaccarino, G., 2003. Toward immersed boundary simulation of high Reynolds number flows. *CTR Annual Res. Briefs*, 369–378.
- Kassinos, S.C., Reynolds, W.C., 1994. A structure-based model for the rapid distortion of homogeneous turbulence, Technical Report TF-61, Mechanical Engineering Department, Stanford University.
- Kassinos, S.C., Langer, C.A., Haire, S.L., Reynolds, W.C., 2000. Structure-based turbulence modeling for wall-bounded flows. *Int. J. Heat Fluid Flow* 21, 599–605.
- Kassinos, S.C., Reynolds, W.C., Rogers, M.M., 2001. One-point turbulence structure tensors. *J. Fluid Mech.* 428, 213–248.
- Kim, J., 1992. Turbulence structure database in channel flow at $Re_\tau = 385$, unpublished.
- Langer, C.A., Reynolds, W.C., 2003. A new algebraic structure-based turbulence model for rotating wall-bounded flows, Technical Report TF-85, Mechanical Engineering Department, Stanford University.
- Lien, F.S., Durbin, P.A., 1996. Non-linear $k-\epsilon-v^2$ modeling with application to high-lift. In: *CTR Summer Proceedings*.
- Moser, R.D., Kim, J., Mansour, N.N., 1999. Direct numerical simulation of turbulent channel flow up to $Re_\tau = 590$. *Phys. Fluids* 11, 943–945.
- Petterson, B.A., Andersson, H.I., 1997. Near-wall Reynolds-stress modelling in noninertial frames of reference. *Fluid Dyn. Res.* 19, 251–276.
- Poroseva, S.V., Kassinos, S.C., Langer, C.A., Reynolds, W.C., 2002. Structure-based turbulence model: application to a rotating pipe flow. *Phys. Fluids* 14, 1523–1532.
- Reynolds, W.C., 1991. Towards a structure-based turbulence model. In: Gatski, T.B., Sarkar, S., Speziale, C.G. (Eds.), *Studies in Turbulence, Lumley 60th Birthday Symposium*. Springer-Verlag, New York, pp. 76–80.
- Reynolds, W.C., Kassinos, S.C., Langer, C.A., Haire, S.L., 2000. New directions in turbulence modeling. In: *The Third International Symposium on Turbulence, Heat, and Mass Transfer*, Nagoya, Japan, April 3–6. Available from: <http://asbm.stanford.edu/asbm.ps>.
- Shih, T.-H., Liou, W.W., Shabbir, A., Zhu, J., 1995. A new $k-\epsilon$ eddy-viscosity model for high Reynolds number turbulent flows. *Comp. Fluids* 24, 227–238.
- Spalart, P.R., 1988. Direct numerical study of a turbulent boundary layer up to $Re_\theta = 1410$. *J. Fluid Mech.* 187, 61–98.
- Spalart, P.R., Watmuff, J.H., 1993. Experimental and numerical study of a turbulent boundary layer with pressure gradients. *J. Fluid Mech.* 249, 337–371.
- Wallin, S., Johansson, A.V., 2002. Modelling streamline curvature effects in explicit algebraic Reynolds stress turbulence models. *Int. J. Heat Fluid Flow* 23 (5), 721–730.
- Wilcox, D.C., 1993. *Turbulence Modeling for CFD*. DCW Industries Inc., La Canada, California.